Altered effective connectivity patterns of the default mode network in Alzheimer's disease: An fMRI study

Yufang Zhong, **Liyu Huang**[*], **Suping Cai**, **Yun Zhang**, **Karen M. von Deneen**, **Aifeng Ren**, and **Junchan Ren Alzheimer's Disease Neuroimaging Initiative**

School of Life Science and Technology, Xidian University, Xi-an, Shaanxi 710071, China

Abstract

The aim of this work is to investigate the differences of effective connectivity of the default mode network (DMN) in Alzheimer's disease (AD) patients and normal controls (NC). The technique of independent component analysis (ICA) was applied to identify DMN components and multivariate Granger causality analysis (mGCA) was used to explore an effective connectivity pattern. We found that: (i) connections in AD were decreased than those in NC, in terms of intensity and quantity. Posterior cingulated cortex (PCC) exhibited significant activity in NC as it connected with most of the other regions within the DMN. Besides, the PCC was the convergence center which only received interactions from other regions; (ii) right inferior temporal cortex (rITC) in the NC exhibited stronger interactions with other regions within the DMN compared with AD patients; and (iii) interactions between medial prefrontal cortex (MPFC) and bilateral inferior parietal cortex (IPC) in the NC were weaker than those in AD patients. These findings may implicate a brain dysfunction in AD patients and reveal more pathophysiological characteristics of AD.

Keywords

Default mode network (DMN); Alzheimer's disease (AD); Independent component analysis (ICA); Multivariate Granger causality analysis (mGCA)

1. Introduction

Alzheimer's disease (AD) is a progressive neurodegenerative disorder which is mainly characterized by significant impairments in a global cognitive decline [2]. It is estimated that half of the population above 80 years old may have symptomatic AD and this number will grow to approximately 81 million by the year 2040 [9]. AD is a widespread epidemic disease threatening social health. However, there is no current effective treatment for this disease [25]. The principal cause of the formation of such a situation is that the pathological mechanism of AD still remains unknown. It would be quite worthwhile to explore the brain activity characteristics from a network perspective.

[*]Corresponding author. Tel.: +86 029 88202261., huangly@mail.xidian.edu.cn (L. Huang).

A number of functional magnetic resonance imaging (fMRI) studies have reported the existence of the default mode network (DMN) and its core regions which mainly include the posterior cingulated cortex (PCC), medial prefrontal cortex (MPFC), inferior parietal cortex (IPC), inferior temporal cortex (ITC) and (para)hippocampus (HC) [3,8]. Viewed as an integrated system, the DMN plays a critical role in monitoring the external environment and supporting internal mentation [10,19]. However, the DMN was frequently found to be abnormal due to AD [1,13,27]. It is totally necessary to investigate how these DMN brain regions interact with each other and the altered causal interaction pattern in relation to AD.

This study combined independent component analysis (ICA) and multivariate Granger causality analysis (mGCA) to investigate the issue of effective connectivity within the DMN in AD patients and normal controls (NC). ICA was successfully used to identify DMN components and mGCA was applied to explore effective connectivity. It is worth noting that our approach of mGCA is quite different from previous implements which were based on the decrease of residual F to evaluate the causal effect [23,24]. Since the residual-based F approximately obeys chi-square distribution, it is a little troublesome in subsequent statistical analysis for group level inference. Our approach applied signed-path coefficients to evaluate the causal effects among brain DMN regions. The signed-path coefficients are considered to be normally distributed and could be used in a parametric statistical analysis at the group level [7]. The use of this model greatly simplifies the subsequent statistical analysis procedure.

2. Materials

2.1. ADNI

Data used in the preparation of this article were obtained from the Alzheimer's Disease Neuroimaging Initiative (ADNI) database (adni.loni.usc.edu/). ADNI was launched in 2003 by the National Institute on Aging (NIA), the National Institute of Biomedical Imaging and Bioengineering (NIBIB), the Food and Drug Administration (FDA), private pharmaceutical companies and non-profit organizations, as a $60 million, 5-year public-private partnership. The primary goal of ADNI has been to test whether serial magnetic resonance imaging (MRI), positron emission tomography (PET), other biological markers, and clinical and neuropsychological assessment can be combined to measure the progression of mild cognitive impairment (MCI) and early AD. Determination of sensitive and specific markers of very early AD progression is intended to aid researchers and clinicians in developing new treatments and monitor their effectiveness, as well as lessen the time and cost of clinical trials.

The Principal Investigator of this initiative is Michael W. Weiner, MD, VA Medical Center and University of California – San Francisco. ADNI is the result of efforts of many co-investigators from a broad range of academic institutions and private corporations, and subjects have been recruited from over 50 sites across the U.S. and Canada. The initial goal of ADNI was to recruit 800 subjects but ADNI has been followed by ADNI-GO and ADNI-2. To date, these three protocols have recruited over 1500 adults, ages 55–90, to participate in the research, consisting of cognitively normal older individuals, people with early or late MCI, and people with early AD. The follow up duration of each group is

specified in the protocols for ADNI-1, ADNI-2 and ADNI-GO. Subjects originally recruited for ADNI-1 and ADNI-GO had the option to be followed in ADNI-2. For up-to-date information, see www.adni-info.org.

2.2.   Subjects

We downloaded 3 T functional MRI data and corresponding clinical data from baseline and follow-up scans from the ADNI publically available database (http://adni.loni.usc.edu/). Thirty-five AD patients (range 63–83 years) and 30 NC (range 65–83 years) were used in this study. The main characteristics of the subjects are reported in Table 1, which presents the baseline clinical and demographic variables of the two groups.

2.3.   Data acquisition

The fMRI data were collected by a 3.0-Tesla Philips MRI scanner. Resting-state functional images were obtained using an echo-planar imaging (EPI) sequence and the parameters included repetition time (TR) = 3000 ms, echo time (TE) = 30 ms, flip angle = 80°, number of slices = 48, slice thickness = 3.3 mm, voxel size = 3 mm × 3 mm × 3 mm, voxel matrix = 64×64 and total volume = 140. All original image files are available to the general scientific community.

2.4.   Data processing

All preprocessing was performed using the Data Processing Assistant for Resting-State fMRI (DPARSF, Yan and Zang, 2010, http://www.restfmri.net), which is based on Statistical Parametric Mapping (SPM8) (http://www.fil.ion.ucl.ac.uk/spm) and Resting-State fMRI Data Analysis Toolkit (REST, Song et al., 2011, http://www.restfmri.net). The first ten time points from each functional image were discarded to allow for equilibration of the magnetic field. All remaining volume slices were corrected for different signal acquisition times. Then, the time series of images for each subject was realigned using a six-parameter (rigid body) linear transformation. Participants with head motion exceeding 1.0 mm in any dimension of x, y and z or 1.0° in any angular motion were excluded for further analysis. The resulting images were then spatial normalized to the standard EPI template with $3 \times 3 \times 3$ resolution. The normalized images were further spatially smoothed with a Gaussian kernel of 6 mm full width at half maximum (FWHM). In order to reduce the effects of confounding factors, the linear trends of time courses were removed using REST. Finally, we applied temporal filtering (0.01 Hz < f < 0.08 Hz) to the time series of each voxel to reduce the effect of low-frequency drifts and high-frequency noise such as respiratory and cardiac rhythms.

3.   Methods

3.1.   ICA

The preprocessed data for all subjects were analyzed with independent component analysis (ICA) for the fMRI toolbox (GIFT, http://icatb.sourceforge.net/) which includes twice principal component analysis (PCA) reduction, ICA separation, and back-reconstruction [5]. Prior to PCA, the optimal number of components was set to 25/30 for NC and AD patients, which was estimated based on minimum description length (MDL). In the first step, data

from each subject were temporally reduced to the optimal number. Then, the reduction step was once again achieved by PCA according to the optimal numbers. In the second step, the data were separated by ICA using the Infomax algorithm [16]. Finally, independent components (ICs) and time courses for each subject were back-reconstructed. The IC that best matched DMN component was selected with a standard DMN template [13]. After the conversion of the intensity values in each IC spatial map to Z-scores, a one sample t-test (height threshold: false discovery rate (FDR), $p = 0.05$, extent threshold: $k = 10$ voxels, $p < 0.01$) was performed to determine the DMN for each of the two groups [6].

3.2. mGCA

Consider the bivariate linear autoregressive model of two time-variant processes $x(t)$ and $y(t)$:

$$x(t) = \alpha_{x,0} + \sum_{i=1}^{p} \alpha_{xx,i} x(t-i) + \sum_{i=1}^{p} \alpha_{xy,i} y(t-i) + \sum_{j=1}^{q} \beta_{x,j} z_j(t) + \varepsilon_x(t)$$

$$y(t) = \alpha_{y,0} + \sum_{i=1}^{p} \alpha_{yx,i} x(t-i) + \sum_{i=1}^{p} \alpha_{yy,i} y(t-i) + \sum_{j=1}^{q} \beta_{y,j} z_j(t) + \varepsilon_y(t)$$

$$(3\text{-}1)$$

where $z_j(t)$ represents up to q exogenous processes (six orthogonal motion estimates and physiological noise) independent of the path network ($j = 1, \ldots q$). Contributions of each lagged variable to the prediction of its respective target are denoted by α; β corresponds to the covariate effect and prediction errors of individual models are denoted by ε. In formulation (3-1), if α_{yx} is significantly different from zero, then it is said that $x(t)$ Granger causes $y(t)$.

The bivariate GCA definition presented in formulation (3-1) can be extended to multivariate conditions (3-2) as well [15].

$$y_1(t) = \alpha_{10} + \sum_{i=1}^{p} \alpha_{11i} y_1(t-i) + \ldots + \sum_{i=1}^{p} \alpha_{1ni} y_n(t-i) + \sum_{j=1}^{q} \beta_{1,j} z_j(t) + \varepsilon_1(t)$$

$$\vdots$$

$$y_n(t) = \alpha_{n0} + \sum_{i=1}^{p} \alpha_{n1i} y_1(t-i) + \ldots + \sum_{i=1}^{p} \alpha_{nni} y_n(t-i) + \sum_{j=1}^{q} \beta_{n,j} z_j(t) + \varepsilon_n(t)$$

$$(3\text{-}2)$$

For each subject, preprocessed time-series data were extracted from peak voxel locations in the regions that showed differential temporals within the DMN between the AD patients and NC. These time-series data for each subject were then entered into mGCA. The resulting path coefficient, characterized by the strength and direction of the temporal relation among the structures, was entered into one-sample t-test ($p = 0.05$, uncorrected) to achieve the group result and further two-sample t-test ($p = 0.05$, uncorrected) to obtain the group differences.

4. Results

4.1. Regions of DMN

We identified eight regions from the DMN map for NC and AD patients separately, detected by ICA and followed by a one-sample t-test with FDR $p = 0.05$. Fig. 1 shows the group DMN results. Since there were no survived voxels at FDR $p = 0.05$ for the bilateral parahippocampal gyrus (PHG) in the AD patients, these two regions were defined with a more lenient threshold of $p = 0.1$, uncorrected. DMN in the NC included the PCC, MPFC, bilateral ITC, IPC and PHG. DMN in AD patients mainly involved the PCC, MPFC, bilateral ITC and IPC.

4.2. Within-group effective connectivity

Fig. 2 shows the effective connectivity patterns learned by mGCA using a one-sample t-test for NC (a) and AD patients (b) respectively. We observed that the connections in AD patients were decreased than those in NC, in terms of both intensity and quantity. PCC was connected with most of the regions within the DMN in NC while exhibiting attenuate interactions in AD patients. In addition, the PCC was the convergence center which only received interactions from other regions.

4.3. Between-group effective connectivity

In order to better evaluate the causal interactions among DMN, we implemented a two-sample t-test between the two groups. Fig. 3 displays the results of DMN causal interactions of NC versus AD patients. We noted that the rITC in NC exhibited stronger interactions with other regions within the DMN. They are connections from the lITC to the lIPC/lPHG/rITC/rPHG (solid line). Besides, interactions between the MPFC and bilateral IPC in NC were weaker than those in AD patients (dashed line).

5. Discussion

This paper applied mGCA combined with ICA to study the effective connectivity patterns in NC and AD patients. In other words, the core regions in the DMN were identified by ICA and were subsequently used to constitute the nodes of mGCA. We noticed that our approach of ICA + mGCA procedure is not conceptually novel. However, the model of mGCA is not the same one as in previous studies [18,29,30]. As mentioned above, the mGCA here used normally distributed signed-path coefficients to evaluate the causal interaction among activated regions. To our best knowledge, this is the first study referencing this model to investigate the configuration of regions within the DMN from the perspective of a causal relationship for NC and AD patients.

We found that connections in AD patients were decreased than those in NC. In another words, some connections were disrupted because of AD. Previous studies on AD have reported decreased functional connectivity in the DMN [13,28]. The abnormal connectivity has been interpreted to be directly related to AD and regarded as the potential biomarker [13,22]. Our results from mGCA were consistent with these findings. What's more, we noted that the PCC was strongly connected with most of the DMN regions while tends to be

attenuate in AD patients. PCC was believed to be the most metabolically active regions in healthy subjects and the most significant functional connectivity region in DMN during resting state [3,14,28]. It is involved in episodic memory function and the most common location appeared in early metabolic and perfusion abnormalities [13]. The decreased interactions may reveal decreased PCC activity which probably was proportional to the declining memory function in AD patients. Thus, the PCC activity could be used as an important clinical index to detect the degree of dementia. In addition, the PCC was the only region which merely received interactions from other regions. We deduced that the PCC may be the most important node of information processing in the DMN. All of the information from other regions must be integrated into the PCC and ultimately exert its function. However, since our research is only limited to the relationship within the DMN, bidirectional interactions may exist between the PCC and other resting state networks [17,18].

It is worth noting that interactions between the rITC and other regions within the DMN were stronger in the NC. That is, the activity of the rITC was inhibited in AD patients. Early evidence has demonstrated that the ITC participates in both visual perception and memory and the rITC is considered to be the repository of long-term visual memory [20]. Most of the AD patients have an obvious decline in memory function [13,17]. The inhibited activity of the rITC, or more generally of the ITC lesion, could be the critical cause of the deficient memory and may reflect a breakdown of visual-related cortical networks in AD patients.

In addition to the reduced interactions within the DMN, increased interactions between the MPFC and bilateral IPC were also observed in AD patients. The MPFC is critical for episodic retrieval and the IPC was recorded to be related to short-term memory [4,26]. Previous studies showed that AD patients presented increased activity in the right dorsal lateral prefrontal cortex (DLPFC), and increased functional connectivity within the prefrontal regions during various memory tasks [11,21]. This increased activity and connectivity have been interpreted to be compensatory recruitment of cognitive resources to maintain task performance [11,12]. The increased interactions between the MPFC and bilateral IPC (prefrontal-parietal lobe) obtained in our study potentially indicate that AD patients possess a relative boost in short-term memory function compared with NC. The enhanced short-term memory well temporarily makes up for its long term memory function defect. With the worsening of the disease, the short-term memory function will eventually be lost. Our findings provided further support that AD patients can make use of additional neural resources in prefrontal regions to compensate for losses of cognitive function.

Acknowledgements

References

[1]. Bai F, Zhang ZJ, Yu H, Shi YM, Yuan YG, Zhu WL, Zhang XR, Qian Y, Default-mode network activity distinguishes amnestic type mild cognitive impairment from healthy aging: a combined structural and resting-state functional MRI study, Neurosci. Lett 438 (2008) 111–115. [PubMed: 18455308]

[2]. Blennow K, de Leon MJ, Zetterberg H, Alzheimer'sdisease, Lancet 368 (2006) 387–403. [PubMed: 16876668]

[3]. Buckner RL, Andrews-Hanna JR, Schacter DL, The brain's default network: anatomy, function, and relevance to disease, Ann. N.Y. Acad. Sci 1124 (2008) 1–38. [PubMed: 18400922]

[4]. Cabeza R, Prince SE, Daselaar SM, Greenberg DL, Budde M, Dolcos F, LaBar KS, Rubin DC, Brain activity during episodic retrieval of autobiographical and laboratory events: an fMRI study using a novel photo paradigm, J. Cogn. Neurosci 16 (2004) 1583–1594. [PubMed: 15622612]

[5]. Calhoun VD, Adali T, Pearlson GD, Pekar JJ, A method for making group inferences from functional MRI data using independent component analysis, Hum. Brain Mapp 14 (2001) 140–151. [PubMed: 11559959]

[6]. Calvini P, Chincarini A, Donadio S, Gemme G, Squarcia S, Nobili F, Rodriguez G, Bellotti R, Catanzariti E, Cerello P, De Mitri I, Fantacci ME, Auto-matic localization of the hippocampal region in MR images to asses early diagnosis of Alzheimer's disease in MCI patients, in: IEEE Nuclear Science Sym-posium Conference Record, 2009, pp. 3622–3628.

[7]. Chen G, Hamilton JP, Thomason ME, Gotlib IH, Saad ZS, Cox RW, Granger causality via vector auto-regression tuned for fMRI data analysis, in: ISMRM 17th Scientific Meeting, Hawaii, 2009.

[8]. Damoiseaux JS, Rombouts SA, Barkhof F, Scheltens P, Stam CJ, Smith SM, Beckmann CF, Consistent resting-state networks across healthy subjects, Proc. Natl. Acad. Sci. U.S.A 103 (2006) 13848–13853. [PubMed: 16945915]

[9]. Ferri CP, Prince M, Brayne C, Brodaty H, Fratiglioni L, Ganguli M, Hall K, Hasegawa K, Hendrie H, Huang Y, Jorm A, Mathers C, Menezes PR, Rimmer E, Scazufca M, Global prevalence of dementia: a Delphi consensus study, Lancet 366 (2005) 2112–2117. [PubMed: 16360788]

[10]. Gilbert SJ, Dumontheil I, Simons JS, Frith CD, Burgess PW, omment on "Wandering minds: the default network and stimulus-independent thought", Science 317 (2007) 43. [PubMed: 17615325]

[11]. Gould RL, Arroyo B, Brown RG, Owen AM, Bullmore ET, Howard RJ, Brain mechanisms of successful compensation during learning in Alzheimer disease, Neurology 67 (2006) 1011–1017. [PubMed: 17000970]

[12]. Grady CL, McIntosh AR, Beig S, Keightley ML, Burian H, Black SE, Evidence from functional neuroimaging of a compensatory prefrontal network in Alzheimer's disease, J. Neurosci 23 (2003) 986–993. [PubMed: 12574428]

[13]. Greicius MD, Srivastava G, Reiss AL, Menon V, Default-mode network activity distinguishes Alzheimer's disease from healthy aging: evidence from functional MRI, Proc. Natl. Acad. Sci. U.S.A 101 (2004) 4637–4642. [PubMed: 15070770]

[14]. Gusnard DA, Raichle ME, Searching for a baseline: functional imaging and the resting human brain, Nat. Rev. Neurosci 2 (2001) 685–694. [PubMed: 11584306]

[15]. Hamilton JP, Chen G, Thomason ME, Schwartz ME, Gotlib IH, Investigating neural primacy in Major Depressive Disorder: multivariate Granger causality analysis of resting-state fMRI time-series data, Mol. Psychiatry 16 (2010) 763–772. [PubMed: 20479758]

[16]. Lee TW, Girolami M, Sejnowski TJ, Independent component analysis using an extended infomax algorithm for mixed subgaussian and supergaussian sources, Neural Comput. 11 (1999) 417–441. [PubMed: 9950738]

[17]. Li J, Li R, Chen K, Yao L, Wu X, Temporal and instantaneous connectivity of default mode network estimated using Gaussian Bayesian network frame-works, Neurosci. Lett 513 (2012) 62–66. [PubMed: 22343026]

[18]. Liu ZY, Bai LJ, Dai RW, Zhong CG, Wang H, You YB, Wei WJ, Tian J, Exploring the effective connectivity of resting state networks in mild cognitive impairment: an fMRI study combining ICA and multivariate Granger causality analysis, in IEEE Engineering in Medicine and Biology, 2012, pp. 5454–5457.

[19]. Mitchell JP, Macrae CN, Banaji MR, Dissociable medial prefrontal contributions to judgments of similar and dissimilar others, Neuron 50 (2006) 655–663. [PubMed: 16701214]

[20]. Miyashita Y, Inferior temporal cortex where visual perception meets memory, Annu. Rev. Neurosci 16 (1993) 245–263. [PubMed: 8460893]

[21]. Pariente J, Cole S, Henson R, Clare L, Kennedy A, Rossor M, Cipoloti L, Puel M, Demonet JF, Chollet F, Frackowiak RSJ, Alzheimer's patients engage an alternative network during a memory task, Ann. Neurol 58 (2005) 870–879. [PubMed: 16315273]

[22]. Raichle ME, MacLeod AM, Snyder AZ, Powers WJ, Gusnard DA, Shulman GL, A default mode of brain function, Proc. Natl. Acad. Sci. U.S.A 98 (2001) 676–682. [PubMed: 11209064]

[23]. Roebroeck A, Formisano E, Goebel R, Mapping directed influence over the brain using Granger causality and fMRI, Neuroimage 25 (2005) 230–242. [PubMed: 15734358]

[24]. Seth AK, Causal connectivity of evolved neural networks during behavior, Network: Comput. Neural Syst 16 (2005) 35–54.

[25]. Shah RS, Lee H-G, Xiongwei Z, Perry G, Smith MA, Castellani RJ, Current approaches in the treatment of Alzheimer's disease, Biomed. Pharmacother 62 (2008) 199–207. [PubMed: 18407457]

[26]. Todd JJ, Marois R, Capacity limit of visual short-term memory in human posterior parietal cortex, Nature 428 (2004) 751–754. [PubMed: 15085133]

[27]. Wang K, Liang M, Wang L, Tian L, Zhang X, Li K, Jiang T, Altered functional connectivity in early Alzheimer's disease: a resting-state fMRI study, Hum. Brain Mapp 28 (2007) 967–978. [PubMed: 17133390]

[28]. Wang L, Zang Y, He Y, Liang M, Zhang X, Tian L, Wu T, Jiang T, Li K, Changes in hippocampal connectivity in the early stages of Alzheimer's disease: evidence from resting state fMRI, Neuroimage 31 (2006) 496–504. [PubMed: 16473024]

[29]. Zhong C, Bai L, Dai R, Xue T, Feng Y, Wang H, Liu Z, You Y, Tian J, Exploring the evolution of post-acupuncture resting-state networks combining ICA and multivariate Granger causality, in: Conference Proceedings: IEEE Engineering in Medicine and Biology Society, vol. 2011, 2011, pp. 2813–2816.

[30]. Zhong CG, Bai LJ, Dai RW, Xue T, Wang H, Feng YY, Liu ZY, You YB, Chen SJ, Tian J Modulatory effects of acupuncture on resting-state networks: a functional MRI study combining independent component analysis and multivariate granger causality analysis, J. Magn. Reson. Imaging 35 (2012) 572–581. [PubMed: 22069078]

HIGHLIGHTS

- The DMN interactions in AD patients were decreased compared with NC.

- PCC was significantly active and had to be the convergence center.

- Region of the rITC exhibited stronger interactions in normal controls.

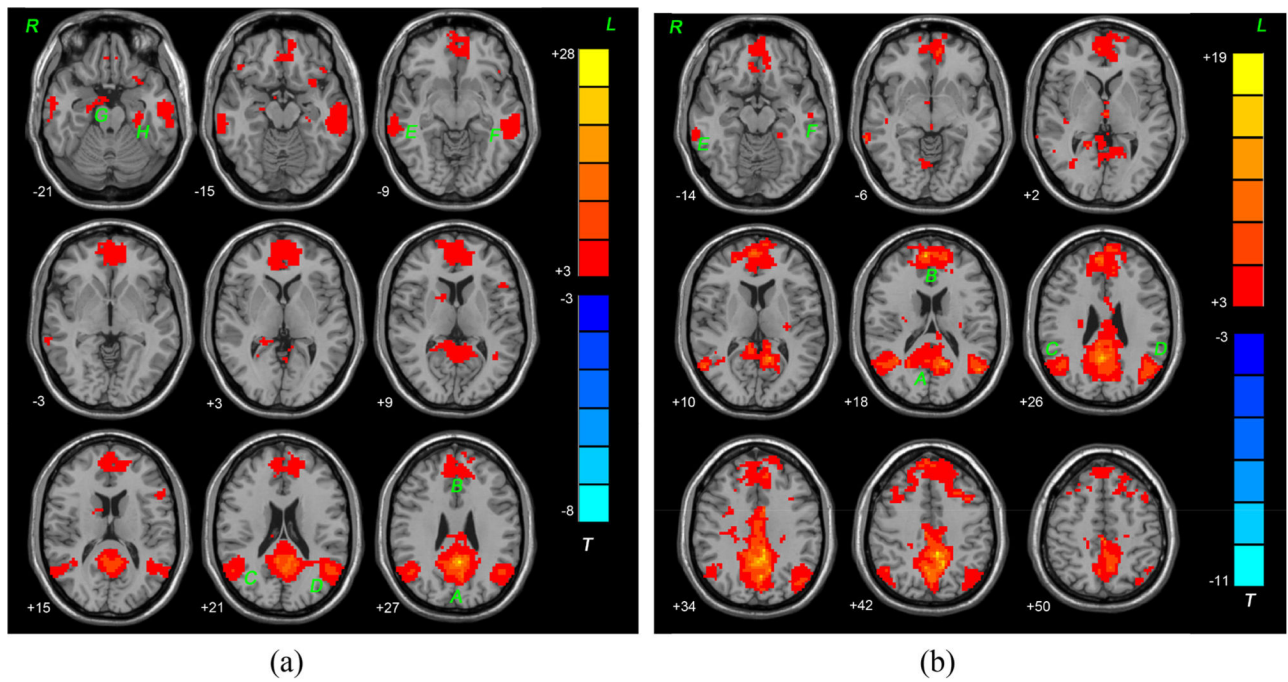- Some interactions in the NC were weaker than those in AD patients.

Fig. 1.
A *T*-statistic map of DMN for normal controls (NC) (a) and AD patients (b). The green capital letters indicate the specific regions in the DMN. *T* score bar is shown on the right (FDR, $p = 0.05$). A: posterior cingulated cortex (PCC), B: medial prefrontal cortex (MPFC), C: left inferior parietal cortex (lIPC), D: right inferior parietal cortex (rIPC), E: left inferior temporal cortex (lITC), F: right inferior temporal cortex (rITC), G: left parahippocampal gyrus (lPHG), H: right parahippocampal gyrus (rPHG).
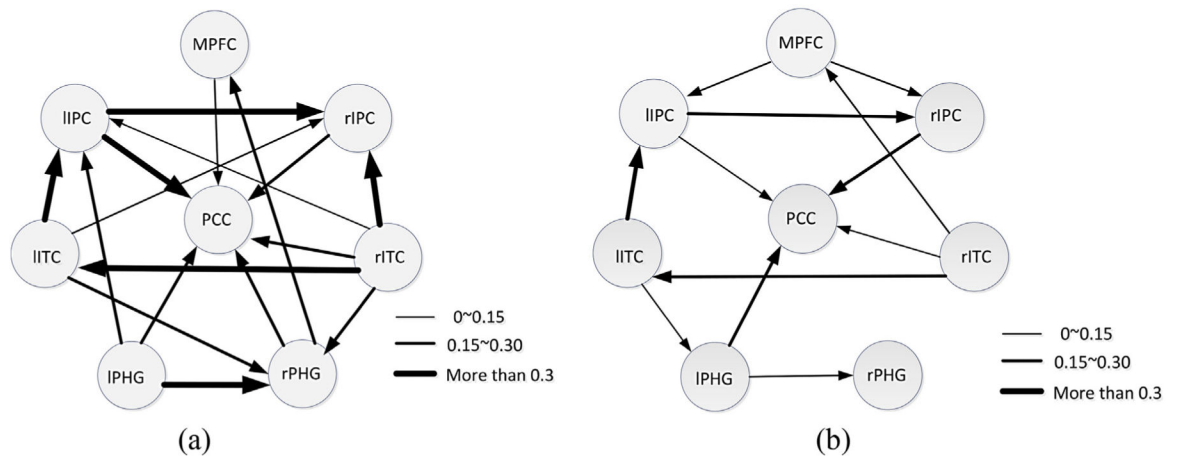
Fig. 2.
T-statistic effective connectivity patterns of DMN in normal controls (a) and AD patients (b). The thickness of the lines is proportional to the connection strength. Connections are tested with significance level $p = 0.05$, one-sample *t*-test.
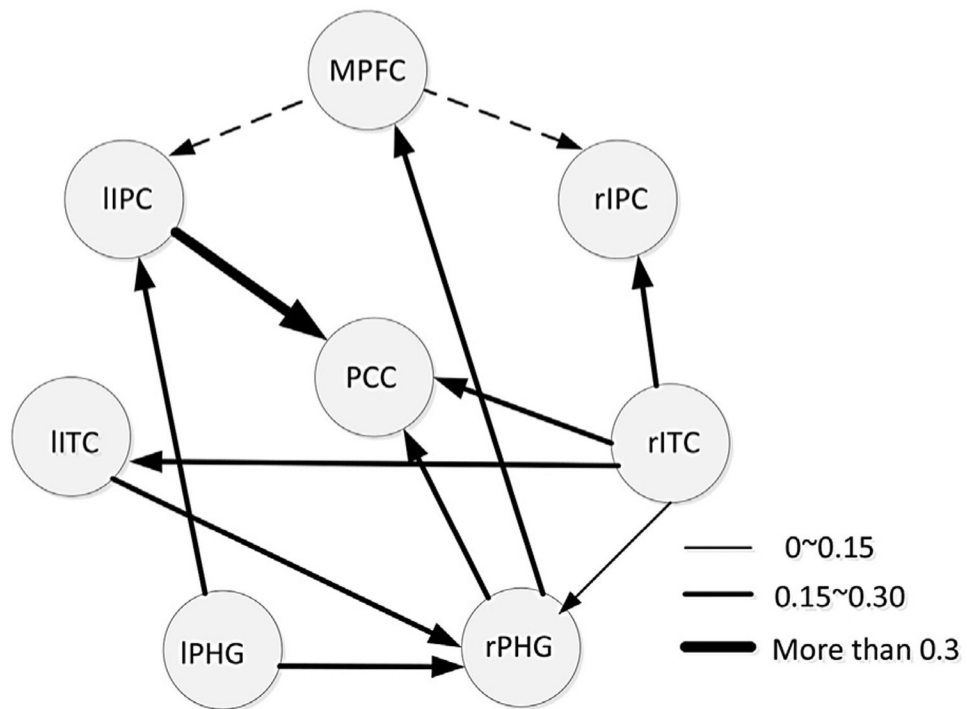
Fig. 3.
T-statistical result of DMN causal interactions of normal controls (NC) versus AD patients. The thickness of the line is proportional to the connection strength. The solid line indicates that the connection in NC is significantly stronger than that in AD patients while the dashed line points out the opposite. Connections are tested with significance level $p = 0.05$, two-sample *t*-test.

Table 1

Demographics and neuropsychological characteristics.

	Age (mean ± SD)	Female/male	MMSE (mean ± SD)	CDR
NC (n = 30)	74.9 ± 5.80	15/15	29.0 ± 1.15	0
AD (n = 35)	72.7 ± 6.76	17/18	21.0 ± 3.52	1

No significant differences ($p < 0.05$) were observed in age or gender between the two groups. Significant differences were noted in MMSE scores between the two groups ($p < 0.0001$).

AD, patients with Alzheimer's disease; NC, normal controls; MMSE, Mini Mental State Examination; CDR, Clinical Dementia Rate.